Transactions, SMiRT-25
Charlotte, NC, USA, August 4-9, 2019
Division V

Beyond Design Earthquake Analyses of Multi-Storey Reinforced Concrete Shear Walls by Use of Shell Element Models within Benchmark CASH Phases 2 and 2B

Michael Borgerhoff[1], Philipp Brede[2], Tadeusz Szczesiak[3] and Urs Bumann[4]

[1] General Manager, Stangenberg & Partners Consulting Engineers, Bochum, Germany (borgerhoff@stangenberg.de)
[2] Structural Engineer, Stangenberg & Partners Consulting Engineers, Bochum, Germany
[3] Dr., Civil Engineering Section, Swiss Federal Nuclear Safety Inspectorate ENSI, Brugg, Switzerland
[4] Head of Section of Structural Engineering, Swiss Federal Nuclear Safety Inspectorate ENSI, Brugg, Switzerland

ABSTRACT

Among the main structural elements of safety-related buildings of nuclear power plants (NPP), the reinforced concrete (RC) walls are particularly important since they carry earthquake induced loads to the foundation. In general this load transfer is dominated by in-plane action, whereby in low-rise walls with a height to width ratio of two or less primarily shear deformations are generated. In comparison with structural elements subjected to bending, the ductility and energy dissipation ability is reduced.

The international benchmarking program on the beyond design seismic CApacity of reinforced concrete SHear walls (CASH) is organised by the OECD NEA (Nuclear Energy Agency). The main objective of the CASH benchmark is to improve the reliability of computer simulations in predicting the capacity of RC shear walls in the case of earthquake actions beyond design basis. The Swiss Federal Nuclear Safety Inspectorate ENSI has participated in the CASH benchmark with two different teams, together with the experts from Stangenberg & Partners Consulting Engineers, Bochum, and from Basler & Hofmann AG, Zürich. In Phase 1 of the CASH benchmark, the participants should calibrate their numerical models using measured values from the SAFE (Structures Armées Faiblement Elancées) experimental program performed by the European Laboratory for Structural Assessment (ELSA), see NECS (2015, 2016) and Labbé et al. (2016). The authors have reported on numerical simulations for Phases 1 and 1B in the last SMiRT conference, see Billmaier et al. (2017) and Borgerhoff et al. (2017).

Subject of this paper are the finite element (FE) analyses carried out in the CASH Phases 2 and 2B, see NECS (2017) and SIXENSE Necs (2018). The objective of these phases is the investigation of seismic nonlinear response of a multi-storey shear wall representative of a real NPP building structure. The simulation results of Phase 2B may be rated as plausible estimates of the capacity of reinforced concrete shear walls and reflect improvements in modelling and computational application due to the insights gained in the previous benchmark phases. The reliability of the calculation method used has thus been confirmed in principle.

HISTORY OF THE CASH BENCHMARK

The CASH benchmark started in 2015 with Phase 1, in which the participants were asked to calibrate their numerical models, see NECS (2015). For this purpose the numerical results could be compared to experimental measurements of tests with low-rise reinforced concrete shear walls performed within the

SAFE experimental program. Due to significant scattering of the results among the participants of Phase 1, the benchmark program has been expanded by Phase 1B, see NECS (2016).

The improved results of Phase 1B served as basis for the numerical analyses in Phase 2 in which two multi-storey shear walls representative of a real NPP building had to be investigated. The basic shape of the symmetric regular structure is modified in the second (irregular) structure by an asymmetrically arranged large wall opening. In total three tasks comprising linear elastic static and seismic modal analyses, nonlinear pushover analyses and linear and nonlinear seismic time history analyses were carried out in Phase 2, see NECS (2017). Such as Phase 1, also Phase 2 was extended by a further phase with updated and unified input parameters and minor modifications in the tasks, which were specified in order to improve the quality and comparability of the results, see SIXENSE Necs (2018). The subsequent description and interpretation of the results is limited to the final Phase 2B.

COMPUTER MODEL

Two structures of the same size are examined by the Finite Element (FE) models shown in Figure 1. The regular structure consists of a four-storey 12 m long wall with 1 m wide flanges representing transversal walls at both ends. The floor height is 4 m. The adjacent ceilings are modelled as 1 m wide beams. In the irregular structure on the third floor level, half of the wall on the right-hand side was removed resulting in a large opening, see Figure 1. All elements of the structure (wall, flanges and ceilings) have a thickness of 0.4 m. With a total height of 16 m and a width of 12 m, the aspect ratio of height to width is 4/3 characterising the structure as low-rise shear wall. In addition to the net weight of the elements, masses of 500 t are considered as only horizontally acting in each ceiling level and of 60 t as only vertically acting.

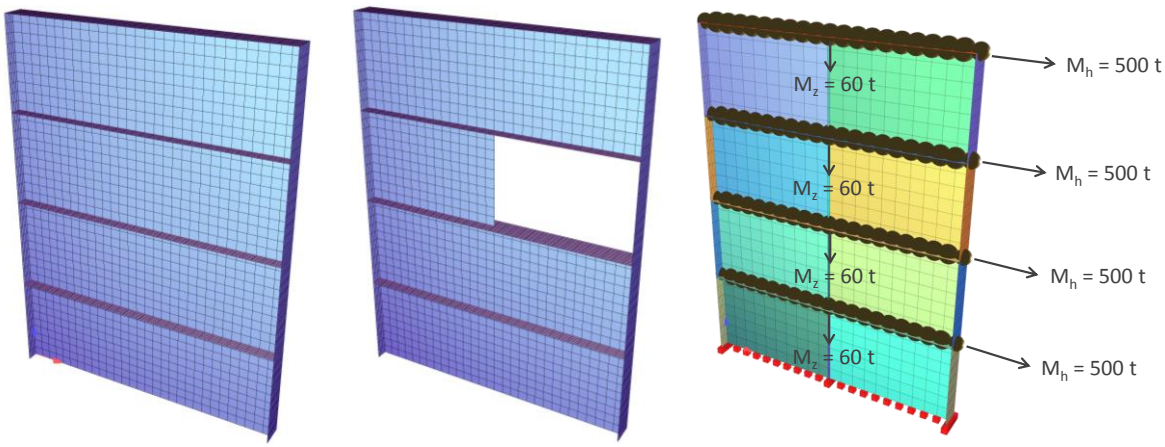

Figure 1. SOFiSTiK FE models in Phase 2B: regular system (left), irregular system (middle) and additional masses acting in horizontal and vertical direction (right).

The numerical analyses of the specimens have been performed by use of the FE computer program SOFiSTiK, which includes a nonlinear reinforced concrete material model, see SOFiSTiK AG (2016). The iterative analysis of nonlinear effects is performed using a modified Newton method with constant stiffness matrix, i.e. an implicit integration scheme is used. The calculation software SOFiSTiK is verified for the linear and nonlinear analysis of RC structures subjected to seismic loads. The reinforced concrete structure is modelled with layered shell elements. A partition into 12 layers is sufficient according to our experience and is used in the performed analyses. Nonlinear shear deformations of the shell/plate elements are approximately included. The nonlinear behaviour of the components of reinforced concrete is defined by

- nonlinear uniaxial stress-strain laws of concrete including hysteretic behaviour (including increase in strength due to biaxial compressive behaviour),
- consideration of tension softening of concrete after cracking dependent on fracture energy with hysteretic behaviour,
- consideration of tension stiffening of reinforcement in the cracked condition,
- approximate inclusion of transverse shear deformations by an elastic/ideally plastic shear stress/shear strain law after exceeding the specified ultimate shear strength and
- tri-linear stress-strain laws of reinforcing steel with hysteretic behaviour.

Besides the wall dimensions and additional masses, steel reinforcement, material properties (see Table 1) and Rayleigh damping coefficients are specified in SIXENSE Necs (2018).

Table 1: Material properties in Phase 2B.

Concrete		Rebar steel	
Compressive strength	f_c = 35 MPa	Young's modulus	E_s = 200 000 MPa
Compression peak strain	ε_c = 2 ‰	Elastic limit	f_e = 500 MPa
Ultimate compressive strain	ε_{uc} = 3.5 ‰	Ultimate tensile strain	ε_{us} = 10 ‰
Young's modulus	E_c = 30 000 MPa	Density	ρ = 7 500 kg/m^3
Tensile limit	f_t = 2 MPa	Hardening modulus	E_h = 1 000 MPa
Ultimate tensile strain	ε_{ut} = 4 f_t / E_c = 0.267 ‰		
Poisson ratio	ν = 0.2		
Density	ρ = 2 300 kg/m^3		
Damping ratio	ζ = 7 % (linear elastic analyses)		
	ζ = 2 % (nonlinear analyses)		

LOCAL MATERIAL TESTS

The CASH benchmark project includes so called "local tests", by which the implementation of the material laws in the computer code is studied on a single element model with dimensions of 1 m × 1 m × 1 m. The two-dimensional square finite element used by the authors has been assigned a thickness of 1 m. For evaluation of the concrete material behaviour under uniaxial and shear loading the single element model was analysed for the load sequences shown in Figure 2. The cyclic uniaxial and shear strains were applied stepwise, and each step was calculated statically. The results plotted in Figure 3 and Figure 4 demonstrate the nonlinear hysteretic material behaviour as implemented in the computer code SOFiSTiK.

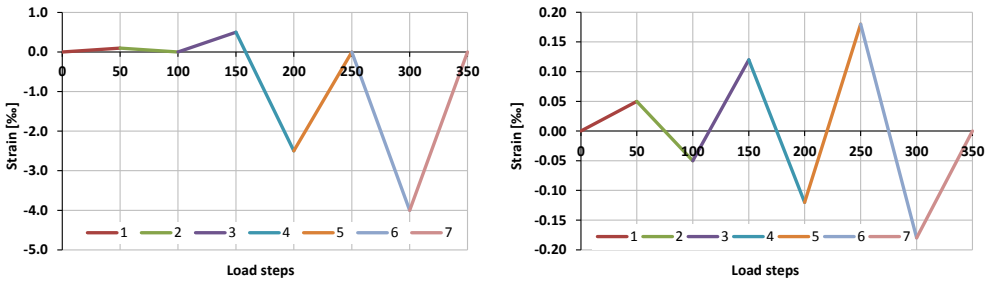

Figure 2. Cyclic load steps for uniaxial behaviour (left) and shear behaviour (right).

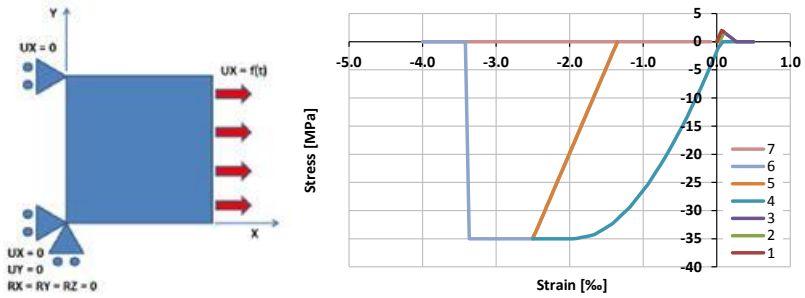

Figure 3. Uniaxial behaviour of concrete, stress vs. strain.

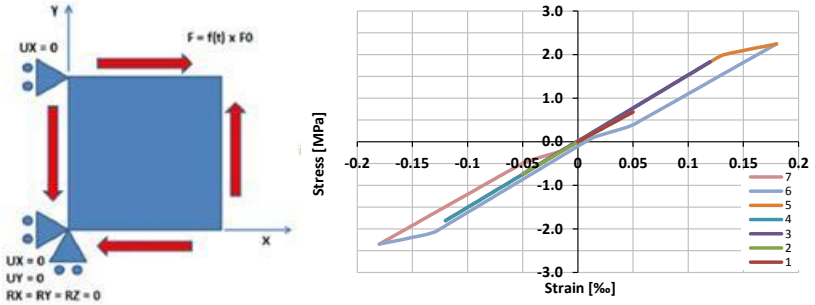

Figure 4. Shear behaviour of concrete, stress vs. strain.

SEISMIC MODAL SPECTRAL ANALYSIS

In the first task of Phase 2B the modal frequencies and the linear response for a given acceleration spectrum had to be determined using the response spectrum method. The calculations have been carried out for both structures with a reduced Young's modulus of E_c = 15 000 MPa in order to approximate the stiffness reduction due to cracking and nonlinear behaviour. The target values of the respective first eigenfrequency 4.1 Hz for the regular system and 3.4 Hz for the irregular system are achieved exactly.

The seismic analyses based on the specified ground response spectrum shown in Figure 5 leads to the maximum horizontal displacements at the centre of the top level of 6.3 mm for the regular and 9.2 mm for the irregular system.

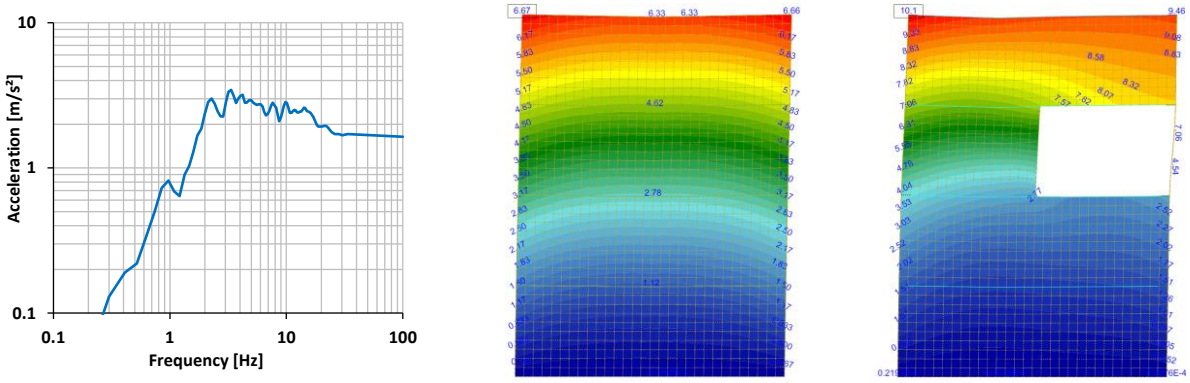

Figure 5. Seismic spectrum and maximum displacements of regular and irregular systems (from left).

NONLINEAR PUSHOVER ANALYSIS

In the second task the behaviour of the two systems under stepwise increasing horizontal force was determined by nonlinear pushover analyses. The applied horizontal force is defined to be proportional to the product of the exclusively horizontally acting nodal masses at the ceiling levels (500 t per floor) and the stepwise increased horizontal displacements, which are compatible with the first eigenmodes of the two FE models.

The horizontal force is increased until the ultimate strains of the materials are exceeded and no equilibrium can be obtained. The ultimate compressive strain of concrete is limited according to specifications in Table 1 by ε_{uc} = 3.5 ‰ and the ultimate tensile strain of steel by ε_{us} = 10 ‰. The full Young's Modulus E_c = 30 000 MPa is used in the pushover analyses. The force is increased gradually until the maximum displacements at the centre of the top level are at least 100 mm. The obtained results are capacity diagrams (base-shear vs. displacements), inter-storey drifts and failure modes of the systems.

Figure 6, Figure 7 and Figure 8 show the deformed shapes at approximately 100 mm horizontal displacement at the centre of the top level of the regular system and the irregular system in positive and negative direction. The crack patterns at approximately 50 mm horizontal displacement in each case shown besides give indications on the expectable failure modes. Along with the largest cracks in the red coloured areas (of the right figures) also large shear deformations can be observed.

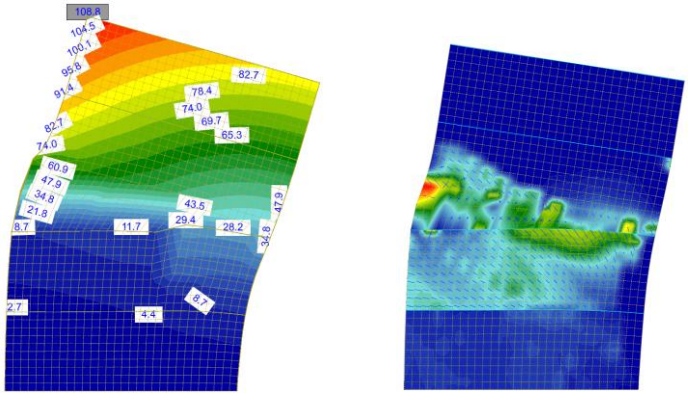

Figure 6. Deformed shape at approx. 100 mm displacement (left) and crack pattern at approx. 50 mm displacement (right) of the regular system.

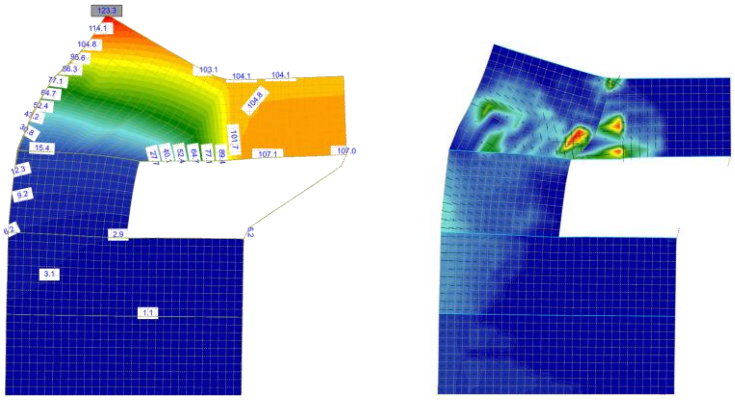

Figure 7. Deformed shape at approx. 100 mm displacement (left) and crack pattern at approx. 50 mm displacement (right) of the irregular system, positive direction.

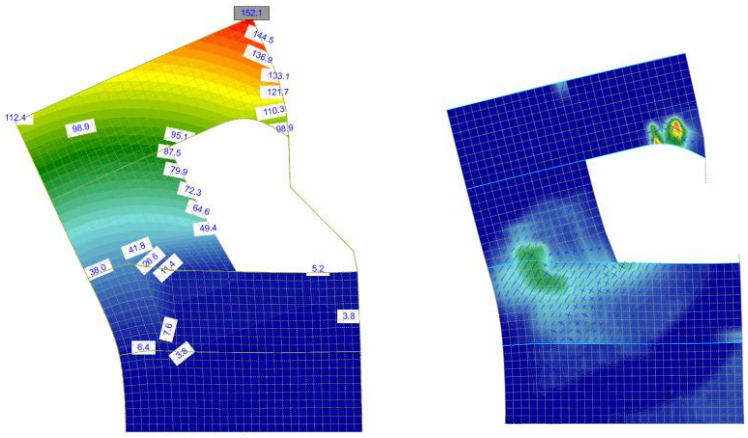

Figure 8. Deformed shape at approx. 100 mm displacement (left) and crack pattern at approx. 50 mm displacement (right) of the irregular system, negative direction.

Estimates of the maximum shear load capacities of the regular and irregular RC shear wall systems can be determined by Figure 9. In this graph the shear force at the base level is plotted against the horizontal displacement at the centre of the top level for both types of structures. Due to the low ultimate tensile strain of the reinforcing steel ε_{us} = 10 ‰, a main failure of the structure due to rupture of the reinforcement is starting already at less than 20 mm horizontal displacement. The interpretation of the results with further increasing horizontal displacements proves to be unfeasible due to the numerical convergence problems associated with the failure of the reinforcement.

The authors therefore consider the specification of ε_{us} = 10 ‰ as failure criterion as unrealistic for the given task and also for later described time history analysis. This problem could be avoided by understanding the parameter only as control value, as done in Hak et al. (2019).

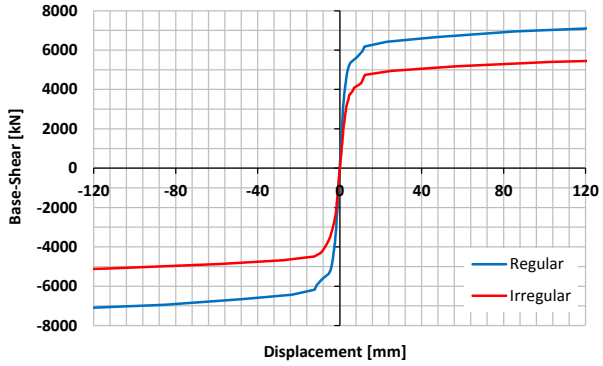

Figure 9. Pushover curves of the regular and irregular systems.

LINEAR AND NONLINEAR SEISMIC TIME HISTORY ANALYSIS

In the third task, linear and nonlinear dynamic analyses of the two types of RC shear walls under a horizontal seismic load with different scaling factors η had to be performed. Figure 10 shows the specified seismic ground motion, which is acting only in horizontal direction. The dead weight of the shear walls is effective in the dynamic analyses together with the additional masses on each floor.

The third task is subdivided into five subtasks, in which the given seismic ground motion was scaled with increasing factors η. In the first, linear analysis, the acceleration time function according to Figure 10 was used in the basic version with factor η = 1 assuming a reduced Young's modulus (E_c = 15 000 MPa) and 7 % damping. In comparison to the first subtask, the second, nonlinear calculation was carried out using the same load, but with the assumption of the full Young's modulus (E_c = 30 000 MPa) and 2 % damping. In the next nonlinear calculation, the scaling factor was increased to η = 2 in order to cause significant damage to the structure. The following subtask was the determination of a factor η_c on condition that 5 ‰ inter-storey drift is reached in one of the 8 resp. 7 partial areas of the shear wall. In the last subtask, the magnification factor η_u should be increased up to the ultimate limit state of the structure, which is defined by the limit strains specified in Table 1.

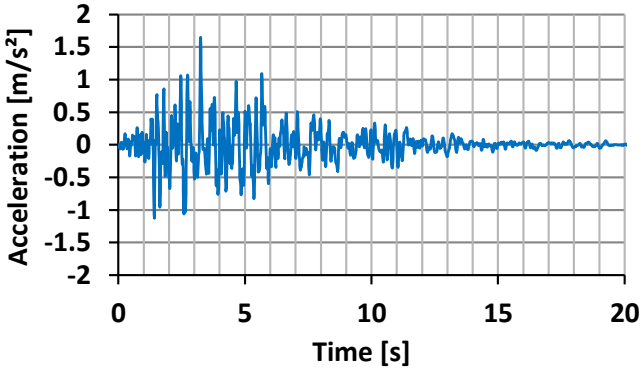

Figure 10. Seismic ground motion (basic version with factor η = 1).

The maximum displacements calculated in the individual subtasks are compiled with the associated time steps in Table 2. The maximum displacements caused by the basic (moderate) seismic excitation with factor η = 1 are much smaller if determined by nonlinear than by linear analysis. This result could be expected considering the fact that the level of seismic excitation is too low to trigger the stiffness reduction due to cracking or plastic deformation. In the case of linear analysis of RC structure (e.g. response spectra analysis) the stiffness reduction must be therefore chosen carefully according to the level of the seismic excitation in order to obtain realistic eigenfrequencies and displacements.

Table 2: Maximum displacements at centre of top level for different factors η.

	Factor η	Displacement [mm]	Time [s]
Regular system	1 (linear)	-6.0	3.3
	1 (nonlinear)	-3.3	4.4
	2	-19.9	3.4
	η_c = 4.5	-40.7	5.9
	η_u = 10	-154	3.9
Irregular system	1 (linear)	-8.1	2.8
	1 (nonlinear)	-6.2	2.8
	2	-19.5	3.4
	η_c = 3	-28.8	3.4
	η_u = 8	86.3	7.6

The default value of 5 ‰ inter-storey drift was achieved for the regular system with a factor of $\eta_c = 4.5$ and for the irregular system with $\eta_c = 3$. The deformed structures of both systems are plotted in Figure 11. Additionally, the crack patterns are shown. In comparison to the pushover analysis results (see Figure 6 to Figure 8), the red coloured areas with the largest cracks and shear deformations in Figure 11 indicate a downwards directed shift of the most stressed wall areas in the dynamic analyses.

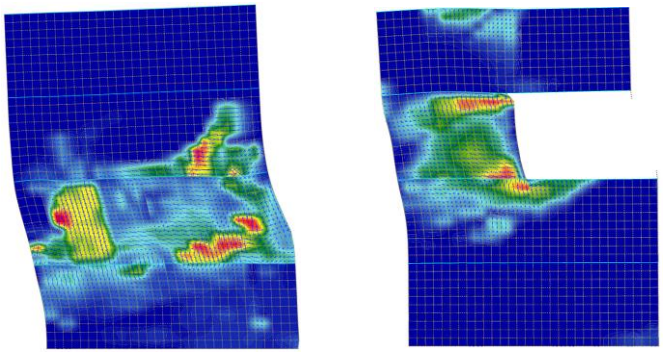

Figure 11. Crack patterns of regular and irregular systems at time of maximum displacements for η_c.

In the parametric analyses for the evaluation of the ultimate capacity factor η_u the seismic load was increased beyond the point, when the ultimate strain limits are achieved for the first time in one single wall location. Due the fact that the steel strain was limited to 10‰ (in accordance with the pushover analysis) the ability of redistribution of the internal forces has been affected. As is apparent from Table 2, the maximum displacements grow disproportionally high with increasing values of η. Thus, the degree of significance of this investigation is questionable.

COMPARISON OF NONLINEAR PUSHOVER AND SEISMIC TIME HISTORY ANALYSES

In order to compare the results of the time history calculations (task 3) with those of the static pushover analyses (task 2), Figure 12 shows the base shear as a function of the horizontal displacement at the centre of the top level for both types of structures. The two diagrams each contain the calculation results for the given seismic time history scaled with different factors η and the pushover curves for both load directions. It turns out that the paths of the base shear from the dynamic calculations are largely enveloped by the pushover curves, especially in the case of the regular system. However, in the course of the cyclic structural behaviour, in particular the pushover curves of the irregular system are exceeded by the dynamic analysis results for the maximum load level of the structure with $\eta_u = 8$. Again the specification of low value of ultimate tensile strain of the reinforcing steel $\varepsilon_{us} = 10$ ‰ has a big impact on the results.

The maximum reaction forces due to the seismic ground motion according to Figure 10 arise in the time period until 6 s. In the diagrams in Figure 13, the force-displacement functions are plotted separately for the time periods until 6 s and > 6 s aiming at a better visibility of the hysteresis loops. The curves for $\eta = 2$ and for η_c (5 ‰ inter-storey drift) except for a small number of oscillations are enveloped by the respective pushover curves.

Primarily, the curves for the regular system clearly show the transition from initially almost linear behaviour to a reduced stiffness due to nonlinear behaviour. The first crack formation takes place within the first second along with displacements of about 1 mm in the regular system and 2 mm in the irregular system. Reinforcing steel plastification begins between 1.5 s and 3 s and related displacements between 9 mm and 11 mm. The ultimate tensile strain $\varepsilon_{us} = 10$ ‰ is reached for the first time after approx. 3 s

linked with displacements of 18 mm in the regular system and 27 mm in the irregular system. The authors consider results up to these displacements as reliable and realistic.

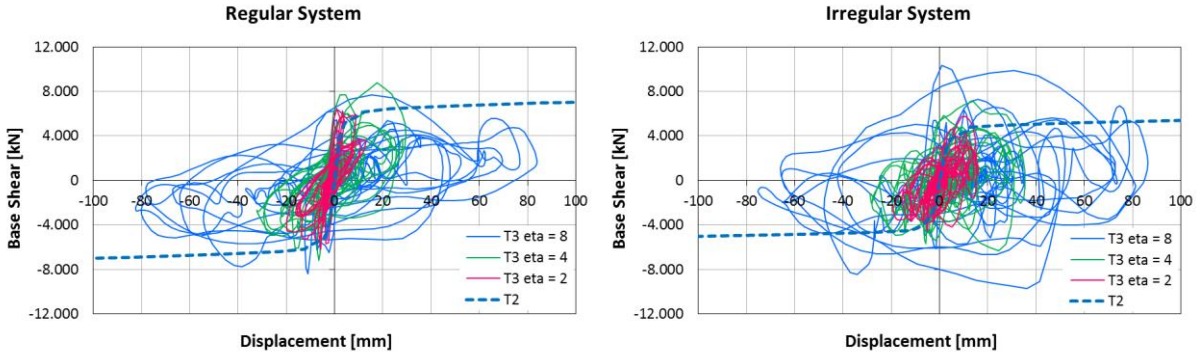

Figure 12. Force-displacement curves of the regular and irregular system for different load levels (T3) compared to the results of the pushover analyses (T2).

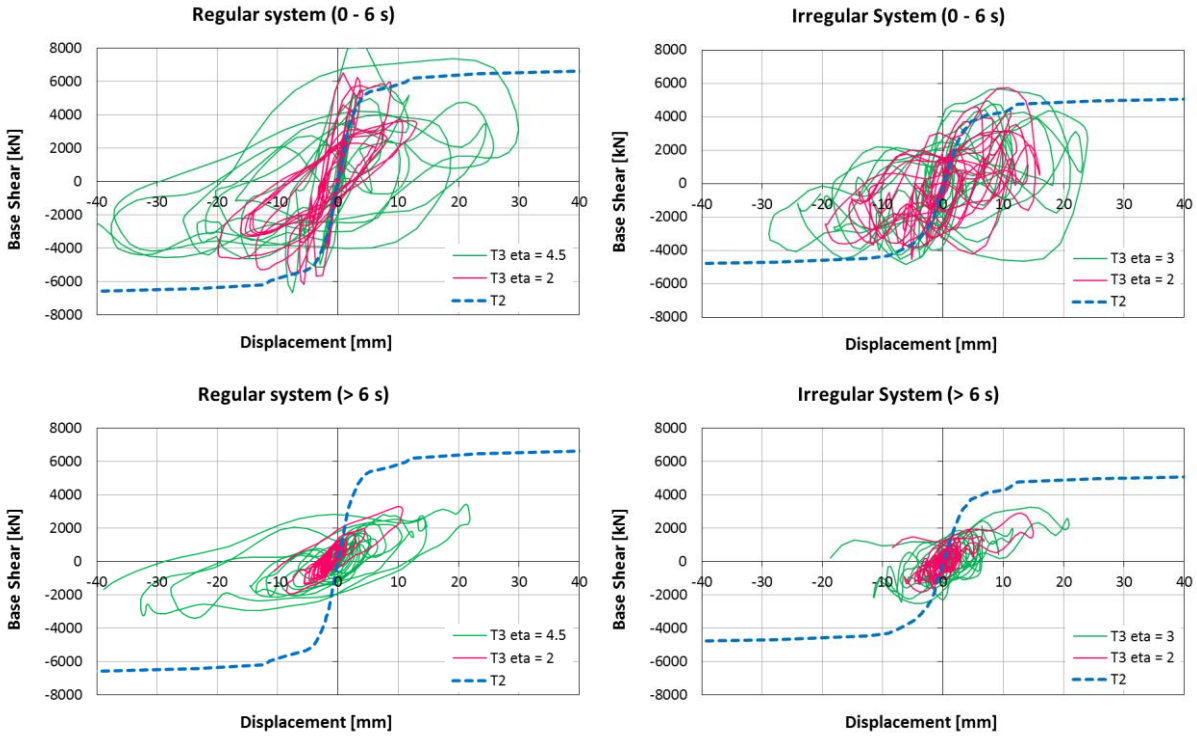

Figure 13. Force-displacement curves of the regular and irregular system separated into the time periods until 6 s and > 6 s.

CONCLUSION

The numerical simulations carried out in the first phases of the CASH benchmark on reinforced concrete shear walls under beyond design earthquake actions have been subject of papers presented by the authors in the SMiRT-24 conference, e.g. Borgerhoff et al. (2017). These investigations have been used to

calibrate the numerical models based on the measured values from tests performed by use of 10 specimens of low-rise shear walls within the SAFE experimental program.

The findings of the first phases were used in the second phase of the CASH benchmark, where the seismic response of two multi-storey reinforced concrete shear walls representative of a real NPP auxiliary building had to be investigated. The insights gained with respect to FE modelling (such as influence of element size, explicit modelling of connected slabs and facades by shell elements) proved to be valuable for reaching the numerical stability of the simulations by use of the FE computer code SOFiSTiK.

The specified (unrealistically low) ultimate tensile strain $\varepsilon_{us} = 10$ ‰ has been interpreted differently in the computations presented in this paper and those reported on in the paper by the other ENSI team participating in the CASH benchmark, see Hak et al. (2019). The assumption of this parameter as failure criterion made here led to a lack of convergence and inconsistent results obtained in the pushover analyses. This problem could be avoided by understanding the parameter only as control value, as done in Hak et al. (2019). It is obvious that the parameter for nonlinear analysis and especially those that influence the failure modes must be chosen carefully.

The influence of the low ultimate tensile strain seems to be less pronounced in the case of nonlinear time history analyses than for pushover analysis in the presented study. The shear force-displacement curves from the dynamic calculations are largely enveloped by the pushover curves, especially in the case of the regular system.

REFERENCES

Billmaier, M., Mondet, Y., Szczesiak, T., Villiger, S., Hak, S. and Bumann, U. (2017). „Squat RC Shear Walls: Beyond Design Seismic Capacity, Lessons Learnt in Benchmark CASH Phase 1 Using LS-DYNA“, *24th Conference on Structural Mechanics in Reactor Technology*, Busan, Korea.

Borgerhoff, M., van Exel, C., Stangenberg, H. and Szczesiak, T. (2017). „Computational Evaluation of Experiments on Seismic Behaviour of Low-Rise Reinforced Concrete Shear Walls”, *24th Conference on Structural Mechanics in Reactor Technology*, Busan, Korea.

Hak, S., Mondet, Y., Szczesiak, T., Rangelow, P. and Bumann, U. (2019). „Beyond Design Seismic Capacity of Squat RC Shear Walls: Lessons Learnt from Phase 2 of the CASH Benchmark Exercise Using LS-DYNA”, *25th Conference on Structural Mechanics in Reactor Technology*, Charlotte, NC, USA.

Labbé, P., Pegon, P., Molina Ruiz, J., Gallios, C., Chauvel, D. (2016). “The SAFE Experimental Research on the Frequency Dependence of Shear Wall Seismic Design Margins”, *Journal of Earthquake Engineering*, Vol 20, Iss. 1.

NECS (2015). *Benchmark CASH, Benchmark on the beyond design seismic capacity of reinforced concrete shear walls, Presentation of the CASH Benchmark Phase 1.* Technical Report, N001_A469_2014_EDF_A.

NECS (2016). *Benchmark CASH, Benchmark on the beyond design seismic capacity of reinforced concrete shear walls, Presentation of the CASH Benchmark Phase 1 B.* Technical Report, N003_A469_2014_EDF_A.

NECS (2017). *Benchmark CASH, Benchmark on the beyond design seismic capacity of reinforced concrete shear walls, Presentation of the CASH Benchmark Phase 2.* Technical Report, N005_A469_2014_EDF_B.

SIXENSE Necs (2018). *Benchmark CASH, Benchmark on the beyond design seismic capacity of reinforced concrete shear walls, Presentation of the CASH Benchmark Phase#2B.* Technical Report, N006_A469_EDF_A.

SOFiSTiK AG (2016). *SOFiSTiK, Analysis Programs,* Version 16.13-33_x64, Oberschleißheim.